Microchemical Journal 140 (2018) 183–188

Contents lists available at ScienceDirect

Microchemical Journal

journal homepage: www.elsevier.com/locate/microc

Quantum chemical computation-based strategy for alternating least squares initialization in multivariate curve resolution analysis of spectral-pH data

Romina Brasca[a,b,c,*], Anne-Marie Kelterer[d,*], Marcel Maeder[e], Mirta R. Alcaráz[a,b], María J. Culzoni[a,b]

[a] Laboratorio de Desarrollo Analítico y Quimiometría (LADAQ), Facultad de Bioquímica y Ciencias Biológicas, Universidad Nacional del Litoral, Ciudad Universitaria, Santa Fe 3000, Argentina
[b] Consejo Nacional de Investigaciones Científicas y Técnicas (CONICET), Godoy Cruz 2290, C1425FQB CABA, Argentina
[c] Programa de Investigación y Análisis de Residuos y Contaminantes Químicos (PRINARC), Facultad de Ingeniería Química, Universidad Nacional del Litoral, Santiago del Estero 2654, 3000 Santa Fe, Argentina
[d] Institute of Physical and Theoretical Chemistry, Graz University of Technology, NAWI Graz, Stremayrgasse 9/Z2, 8010 Graz, Austria
[e] Department of Chemistry, University of Newcastle, University Drive, Newcastle 2308, Australia

ARTICLE INFO

Keywords:
Molecular absorption spectroscopy
Multivariate curve resolution - alternating least squares
Time-dependent density functional theory
Initial estimates

ABSTRACT

The main motivation of this work is to provide initial estimates for the initialization of the iterative optimization within the multivariate curve resolution - alternating least squares (MCR-ALS) algorithm for the decomposition of second-order data. It is demonstrated that the combination of quantum chemical calculations with chemometrics constitutes a novel strategy for the ALS initialization in the MCR resolution of pH-modulated chemical data. In this work, the second-order data arise from acid-base experiments of *p*-nitrophenol (pNP) done under a pH-gradient generated by an automated flow injection (FI) system monitored by UV–vis spectroscopy. The absorption spectra of the species involved in the chemical equilibrium were simulated by means of time-dependent density functional theory (TD-DFT) methods and were utilized to start the ALS optimization. The new approach based on the Tamm-Dancoff-approximation (TDA) CAM-B3LYP method is recommended to obtain the simulated spectra to initialize MCR-ALS, as an alternative to the routinely methods used to generate initial estimates.

1. Introduction

Multivariate curve resolution - alternating least squares (MCR-ALS) is an iterative soft-modeling method that allows obtaining qualitative and quantitative information about a multicomponent system by discerning the individual contribution of the underlying components [1–4]. This algorithm has been used in several research fields and has demonstrated its applicability in various experimental methodologies that generate second-order data by using hyphenated techniques, e.g., chromatographic methods coupled to spectrophotometric detection [5,6], or in spectrophotometric monitoring of chemical reaction kinetics [7–9] or titration experiments [10].

It is known that MCR-ALS requires initialization of the iterative process using initial estimates on spectral or concentration profiles. Examples of methods that offer initial estimations for MCR-ALS are the simple interactive self-modeling mixture analysis (SIMPLISMA) [11] and evolving factor analysis (EFA) [12].

It is well accepted that quantum chemical calculations based on time-dependent density functional theory (TD-DFT), using suitable functionals and solvation models, can be properly applied to describe the absorption spectra of a variety of organic compounds in reasonable agreement with experiments [13,14]. In this sense, in a previous publication, a TD-DFT methodology was applied to calculate the absorption spectra of antihistaminic drugs in order to explain the influence of the stepwise protonation on the experimental spectra [15]. It was demonstrated that the TD-CAM-B3LYP method, combined with a continuum solvation model, performed well on the calculation of the spectra of the acid-base species.

Therefore, as a continuation of the aforementioned study, we decided to explore the feasibility of using TD-DFT simulated spectra as initial estimates for the ALS iteration in MCR analysis of spectrophotometric titration experiments, as an alternative strategy for initialization. In order to benchmark the computational simulation against the commonly implemented initialization methods, the resolution using TD-DFT simulated spectra was compared with those obtained from the SIMPLISMA-based algorithm and EFA. To favor this analysis,

* Corresponding authors.
E-mail addresses: rbrasca@fiq.unl.edu.ar (R. Brasca), kelterer@tugraz.at (A.-M. Kelterer).

https://doi.org/10.1016/j.microc.2018.04.022
Received 13 March 2018; Received in revised form 16 April 2018; Accepted 17 April 2018
Available online 18 April 2018
0026-265X/

p-nitrophenol (pNP) was chosen as a case study since it is a simple organic compound which displays notable changes in the absorption spectra by virtue of its acid-base properties. To the best of our knowledge, this is the first time that TD-DFT simulated spectra serve as input data for chemometric modeling of acid-base equilibrium by MCR-ALS.

2. Experimental

2.1. Reagents and solutions

pNP was synthesized by nitration of phenol [16] and purified by recrystallization [17] following the procedures described in the literature. Methanol (MeOH) LC grade was obtained from LiChrosolv (Merck Millipore Co., Darmstadt, Germany). Sodium phosphate dibasic dihydrate ($Na_2HPO_4{\cdot}2H_2O$) and sodium hydroxide (NaOH) were obtained from Anedra (La Plata, Argentina). Phosphoric acid 85 wt% (H_3PO_4) was purchase from Cicarelli (San Lorenzo, Argentina). Ultrapure water used for the preparation of all solutions was obtained from a Milli-Q water purification system from Millipore (Bedford, USA).

A stock solution of pNP at a concentration of 37 mmol L^{-1} was prepared by dissolving the appropriate amount of the drug in slightly alkaline ultrapure water, and then stored at 4 °C in an amber flask. Working solutions at concentration of 0.1 mmol L^{-1} of pNP were daily prepared by dilution of the stock solution in 0.1 mol L^{-1} phosphate buffer at pH 2.0 or 9.0, as appropriate.

For the FI analysis measurements, a 0.1 mol L^{-1} phosphate buffer pH 2.0 was prepared by transferring an appropriate volume of H_3PO_4 85 wt% to a 250.00 mL volumetric flask, adjusting the pH to 2.0 with 1.0 mol L^{-1} NaOH, and completing to the mark with ultrapure water. 250.00 mL of a 0.1 mol L^{-1} phosphate buffer pH 9.0 were prepared by dissolving the suitable amount of $Na_2HPO_4{\cdot}2H_2O$ in ultrapure water, adjusting the pH to 9.0 with 1.0 mol L^{-1} NaOH, and completing to the mark with ultrapure water.

2.2. Apparatus

A flow injection (FI) system was set using a five modules (degasser, pump, injection valve, autosampler and a diode-array detector) Agilent 1100 Series LC instrument (Agilent Technologies, Waldbronn, Germany). The carrier buffer was pumped through an 800 mm length and 0.5 mm inner diameter flexible coil at a flow rate of 0.4 mL min^{-1}. Absorption spectra were registered in the range of 250–500 nm every 2 nm at regular steps of 0.4 s in a period of 57 s.

The pH of the solutions was measured with an Orion (Massachusetts, USA) 410 A potentiometer equipped with a Boeco (Hamburg, Germany) BA 17 combined glass electrode.

2.3. Software and simulations

Data processing and MCR-ALS analysis were performed in MATLAB 7.10. MCR-ALS algorithms were implemented by using the graphical interface available at http://www.mcrals.info.

Geometry optimizations of the neutral and deprotonated species of pNP were performed in gas-phase at DFT level of theory using the B3LYP [18] functional with def2-TZVP [19] basis set (method M1). Resolution of identity approach to second-order Møller-Plesset perturbation theory (RI-MP2) [20–22] was additionally tested together with the def2-TZVPP basis set (method M2). All geometries were verified as true minimum by frequency calculations. Calculations of vertical excitations were carried out at the ground-state optimized geometries using the Tamm-Dancoff-approximation TDA-DFT as implemented in GAMESS [23], i.e., CAM-B3LYP functional [24] and def2-TZVPP basis set. To emulate water medium, the conductor-like screening model (COSMO) [25,26] was applied for the optimizations as implemented in the program ORCA [27], and for the excitations the analogue conductor-like polarizable continuum model (C-PCM) [28,29] was applied as implemented in GAMESS. The calculated electronic transitions correspond to the first 10 excitations. Absorption spectra were convoluted from the vertical excitations invoking the orca_asa program [30,31] using the Simple Model. For all the transitions, Gaussian lineshapes with a specific broadening (σ) were implemented to mimic the experimental absorption spectra. Considering that DFT functionals intrinsically have systematic errors for π-π* and charge-transfer transitions (about 0.31 eV and 0.86 eV, respectively) [32–34] shifting the spectra by an appropriate value is a way to improve the simulation performance. Additionally, the half width at half height (HWHH) is a parameter influencing the shape of the simulated spectra. It is a common practice in the DFT community to apply appropriate HWHH and shifting the convoluted energies to get the best possible agreement with experimental spectra.

2.4. Spectral-pH data acquisition

To perform the pH-dependence measurements a pH-gradient FI system with diode-array detection (DAD) was used. 50 µL of pNP working solution prepared at pH 9.0 were injected into an acid carrier stream (pH 2.0), producing a dispersive gradient along the time. In this way, a data matrix with a size of 143 × 126 was obtained for the temporal and spectral dimension, respectively (Fig. 1).

Reference absorption spectra of pure species were obtained from experiments done at selected pH conditions: pH 2.0 and 9.0 for the neutral and anionic forms of pNP, respectively. In this way, non-pH-gradient measurements were performed by preparing the sample and the carrier at the same pH value. Subsequently, the reference spectra of pure pNP species were obtained from the corresponding data matrix at 0.21 min.

2.5. Chemometric analysis

MCR-ALS algorithm decomposes second-order data sets (**D**) achieving a bilinear measurement model into the product of two smaller matrices, **C** and **S**, which contain the information of the components involved in the system, and one matrix **E** that comprises the error contribution to the measurement [1]. In the case of spectral-pH data, each column of **C** would contain the concentration of each species present in the system and the rows of $\mathbf{S}^T$ their related spectra. The bilinear decomposition Eq. (1) could be written as follow:

$$\mathbf{D} = \mathbf{C} \times \mathbf{S}^T + \mathbf{E} \quad (1)$$

In this work, MCR-ALS was applied to obtain the individual contributions of every component involved in the acid-base equilibrium. The bilinear decomposition allowed revealing the spectral profile of each species and its abundance contribution along the evaluated pH

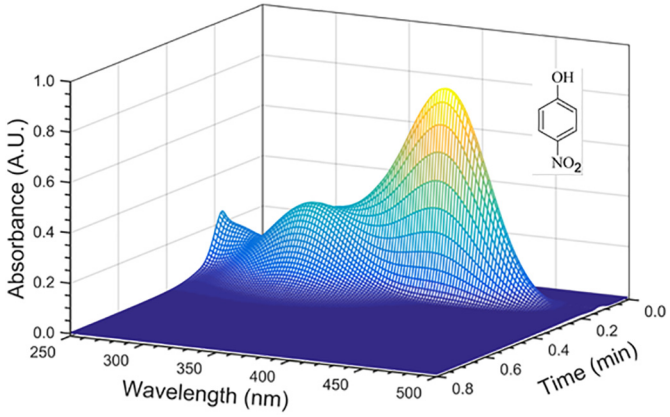

Fig. 1. Three-dimensional representation of experimental data for pNP obtained by the FI system.

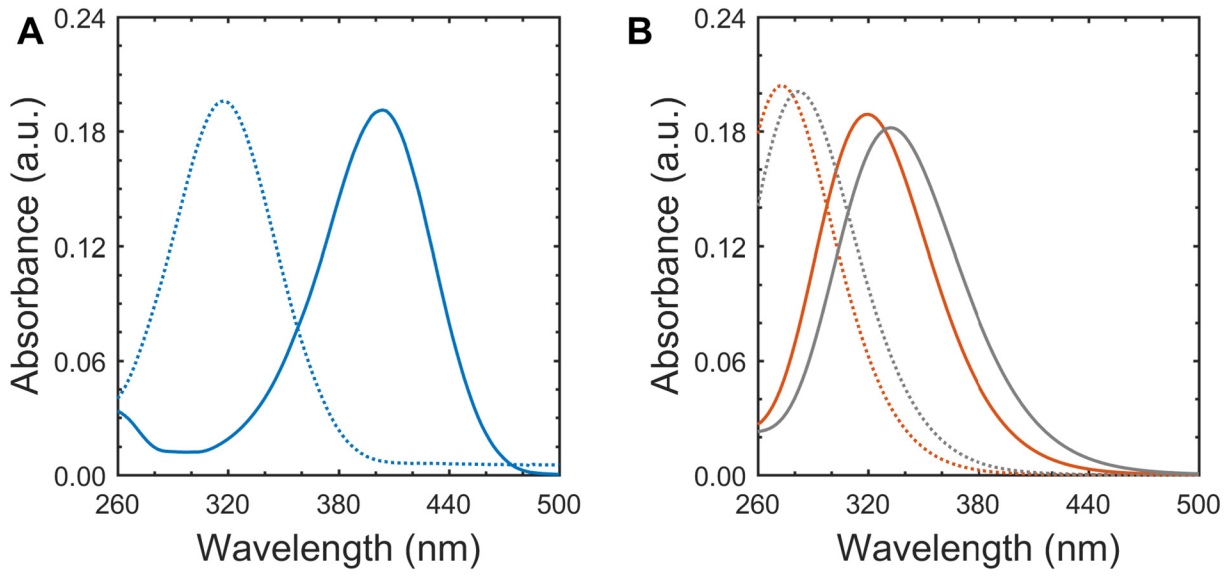

Fig. 2. Normalized electronic spectra of pNP in acid (dotted lines) and alkaline (solid lines) media conditions obtained by (A) experimental measurements (blue lines) and (B) TDA-CAM-B3LYP/def2-TZVPP computational simulations using Gaussian lineshapes with σ = 3000 cm^{-1} without (red lines) and with (gray lines) shifting of 1200 cm^{-1}. (For interpretation of the references to colour in this figure legend, the reader is referred to the web version of this article.)

range. Then, a comparison between the spectral profiles obtained by MCR-ALS and the reference spectra were carried out, and the similarity coefficient *r* (Eq. 2) [35,36] was calculated as follow:

$$r = \frac{\|\mathbf{s}_1^T \mathbf{s}_2\|}{\|\mathbf{s}_1\| \|\mathbf{s}_2\|} \quad (2)$$

where $\mathbf{s}_1$ is the reference spectra of the pure species and $\mathbf{s}_2$ is the corresponding spectral profile retrieved by MCR-ALS.

3. Results and discussion

3.1. Spectroscopic behavior in different aqueous medium conditions

It has been demonstrated that in acidic aqueous pNP solutions a maximum absorption intensity at 317 nm is observed, which then decreases as the pH increases, and simultaneously a new band with a maximum absorption intensity at 400 nm arises [37,38]. In acid conditions the neutral form (pNPn) predominates over the anionic form (pNP^-), which is present at alkaline conditions. In Fig. 2.A the experimental spectra of pNP species are shown.

3.2. Simulation of the absorption spectra by TD-DFT methods

The deprotonation of the hydroxyl substituent of pNP generates a remarkable spectral change that can be clearly seen in the simulated spectra (Fig. 2.B). After applying a broadening of 3000 cm^{-1} for the convolution of the absorption spectra, a maximum intensity at 274 nm and 320 nm are observed for the simulated spectra of the neutral and deprotonated species, respectively. The computational results indicate that the molecular orbitals that contribute to these dominant transitions are the HOMO and the LUMO (π-π* type) of pNPn and pNP^-, respectively.

Several computational approaches were evaluated to achieve the best agreement of the peak positions between experimental and simulated spectra (Table 1). For example, new geometry optimizations with RI-MP2/def2-TZVPP were performed, the popular B3LYP functional for calculations of the vertical excitation energies was also tested and explicit solvent molecules were added to the continuum solvent calculations (one water molecule and one hydronium ion were added to pNPn and pNP^-, respectively). As can be seen in Table 1, when the differences of the maximum absorption positions for the neutral and deprotonated forms are compared, the TDA-CAM-B3LYP functional leads to the best agreement of the calculated with the experimental spectra. Since the addition of explicit solvent molecules did not improve the agreement between the calculations and experiments, TDA-CAM-B3LYP spectra simulated without inclusion of solvent molecules was selected for computations on pNP species.

Table 1
Difference between maximum intensity positions of the absorption spectra of pNP^- and pNPn for simulations carried out using different computational approaches and a broadening of 3000 cm^{-1}.

Simulation method in water			$(\lambda_{max}^{pNP-} - \lambda_{max}^{pNPn})$	
Vertical excitation	Optimization[a]	Solvent model	eV	nm
TDA-CAM-B3LYP/def2-TZVPP/C-PCM	M2	Continuum	0.71	51
	M1	Continuum	0.67	47
	M1	Explicit solvent[b]	0.46	33
TDA-B3LYP/def2-TZVPP/C-PCM	M2	Continuum	0.38	30
	M1	Continuum	0.31	24
	M1	Explicit solvent[b]	0.25	20
Experiment			0.83	86

[a] M1 = B3LYP/def2-TZVP/COSMO; M2 = RI-MP2/def2-TZVPP/COSMO.
[b] One water molecule and one hydronium ion were added to pNPn and pNP^-, respectively.

Additionally, other computational approaches were tested using the TDA-CAM-B3LYP simulated spectra as initial estimates. For this purpose, the spectra were convoluted using broadenings of 1500 and 2000 cm^{-1}, and a shift of 1200 cm^{-1} to longer wavenumbers was applied to compensate the systematic errors of CAM-B3LYP.

Finally, TDA-CAM-B3LYP spectra convoluted using a broadening of 3000 cm^{-1} and shifted by 1200 cm^{-1} ($\boldsymbol{\lambda}_{max}^{\boldsymbol{pNPn}}$ = 282 nm and $\boldsymbol{\lambda}_{max}^{\boldsymbol{pNP-}}$ = 332 nm) were selected as estimates for the initialization of the iteration process in ALS optimization (Fig. 2.B).

3.3. MCR-ALS analysis using different initialization strategies

Prior to MCR-ALS analysis, the number of contributing components was estimated by applying singular value decomposition (SVD) [39].

For ALS initialization, different strategies were utilized in order to obtain initial estimates. First, auxiliary chemometric algorithms were used to generate the initial estimates, such as the purest component spectra by using a methodology based on SIMPLISMA or the concentration evolution of each component by applying EFA. Besides, initialization with spectra of pure components was carried out by using the reference absorption spectra obtained from experiments done at the corresponding pH values (Fig. 2.A). Finally, normalized spectra obtained by computational simulations with the TDA-CAM-B3LYP functional were employed. With this aim, different sets of TDA-CAM-B3LYP//M1 and TDA-CAM-B3LYP//M2 simulated normalized spectra were used to build the initial estimates.

The MCR-ALS decomposition of a data matrix is not unique since different mathematical solutions will fit the experimental data equally well but they will be different from a chemical point of view. Therefore, the incorporation of certain constraints to the ALS optimization, such as non-negativity, closure, selectivity, among others, reduces the range of feasible solutions [2]. In addition, the resolution can be improved if extra information of the pure components is available [40]. In this work, in order to minimize the ambiguity of the chemometric resolution, the ALS optimization was performed applying the non-negativity constraint in both the spectral and concentration modes. Additionally, the closure constraint was imposed considering the mass-balance of the total concentration in the reacting system. Therefore, peak shape concentration closure was implemented to fulfil the sample dispersion profile. The closure vector was taken from the concentration mode on the original data matrix at the isosbestic wavelength of 358 nm, at which the absorbance of pNPn and pNP^- are essentially independent of pH, and therefore the concentration at each point is the sum of the contribution of both species.

To show the effect of the initial estimates in the MCR-ALS resolution, the spectral and time profiles of the chemical species participating in the pNP equilibrium retrieved by the different MCR-ALS analyses were compared with the reference data.

First, the matrices of pure pNPn and pNP^- species obtained by non-pH-gradient procedure were analyzed by MCR-ALS. The number of components obtained by applying SVD to pH 2.0 data matrix was 2, and only 1 component was necessary to explain the variance of the system for the pH 9.0 data matrix. After MCR-ALS resolution, an inspection of the retrieved profiles allowed to attribute these contributions to the acid species and the background contribution in the first case, and basic species in the second case. Background contributions were also encountered in earlier studies for similar systems and they have been ascribed to the absorption of the components of the buffer [41–43]. In accordance, the number of components obtained from the pH-gradient data matrix by SVD was 3 (pNPn, pNP^- and the background contribution). Subsequently, the data matrix of the pNPn/pNP^- equilibrium obtained by the pH-gradient procedure was analyzed by MCR-ALS. The spectral and time profiles of the acid and basic species are presented in Fig. 3.A and .B, respectively.

When the initialization was performed by using the spectral profiles extracted by means of SIMPLISMA-based algorithm, the pNPn spectral profile obtained presents excellent agreement with the reference spectrum of the neutral species, exhibiting its maximum absorption intensity at 318 nm (Fig. 3.A). However, even though the retrieved profile of the deprotonated compound pNP^- shows the characteristic main peak, with its maximum absorption position at 404 nm, an extra band at lower wavelengths (~320 nm) appears, which is not observed in the experimental reference spectrum. On the other hand, the initialization of MCR-ALS resolution with initial estimates obtained by EFA retrieves profiles equivalent to the reference spectra of the pure components, with only a slightly difference between spectra corresponding to the neutral species (Fig. 3.A).

Finally, the spectral profiles retrieved after initialization with the shifted simulated normalized spectra, using TDA-CAM-B3LYP//M1 (or M2) functional with a broadening of 3000 cm^{-1}, present an excellent

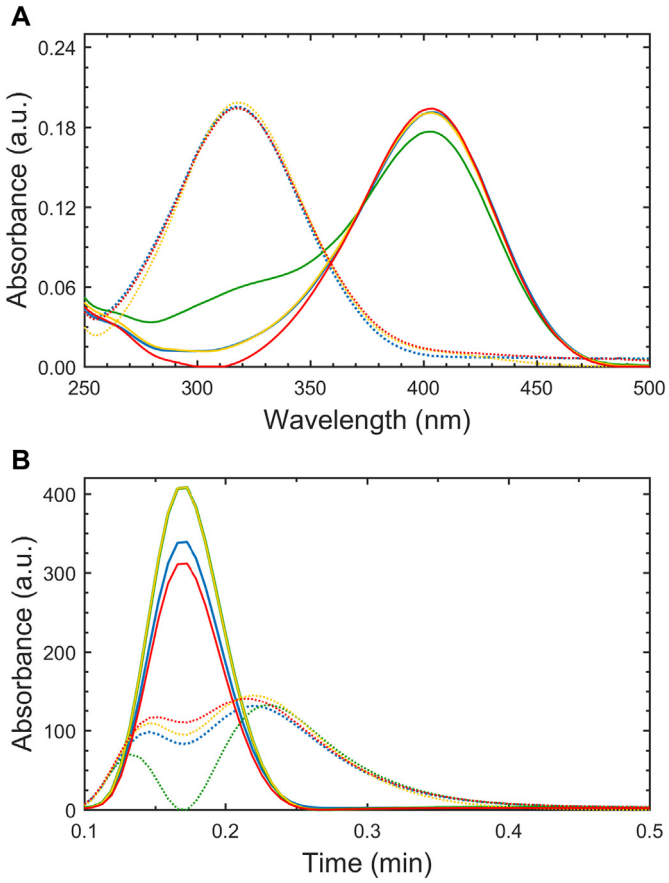

Fig. 3. (A) Spectral and (B) time profiles retrieved for pNPn (dotted lines) and pNP^- species (solid lines) by MCR-ALS analysis of pH-gradient spectrophotometric data using profiles extracted from SIMPLISMA-based algorithm (green lines), EFA (dashed yellow lines) and TDA-CAM-B3LYP simulated shifted normalized spectra (red lines) as initial estimates. Blue lines represent (A) the reference spectra and (B) the time profiles recovered by MCR-ALS resolution after initialization with reference spectra of pure components. (For interpretation of the references to colour in this figure legend, the reader is referred to the web version of this article.)

agreement with the reference spectra of the pure components for the neutral species, with a minor difference between the spectra that correspond to the anion (Fig. 3.A). Here, the matrix containing the initial estimates was built with the two simulated spectra corresponding to the pNPn/pNP^- equilibrium and a third component that represents the background contribution, which was obtained from the decomposition with the SIMPLISMA-based algorithm.

Thus, the best spectral overlaps were observed for pNP species when the initial estimates are obtained from EFA algorithm and TDA-CAM-B3LYP simulations (Table 2). On the contrary, the initialization with SIMPLISMA-based algorithm estimates led to the lowest degree of overlap between spectra.

The time profiles of pNPn and pNP^- species obtained by MCR-ALS (Fig. 3.B) show the characteristic shape of a pH-gradient resulting from

Table 2
Similarity coefficient *r* between reference absorption spectra of pure pNP species and spectral profiles retrieved by MCR-ALS by using different initial estimates.

Initial estimates obtained from	pNPn	pNP^-
SIMPLISMA-based algorithm	0.9993	0.9761
EFA algorithm	0.9978	0.9998
TDA-CAM-B3LYP simulations	0.9993	0.9977

the injection of a discrete bolus of the alkaline sample into the acidic carrier solution [43–45]. In this case, a double pH-gradient is generated after injection showing a maximum acidity in the boundaries of the sample bolus and an alkaline media zone in the center of the FI peak.

In all cases, the time profiles obtained after the bilinear decomposition present similar characteristics, except for the case of initialization with the estimates obtained by SIMPLISMA-based algorithm. The main difference lies in the concentration distribution of the acid species in the center of the sample bolus, where the basic species predominates. In Fig. 3.B, it can be appreciated that the concentration of the acid species decreases in the center of the bolus leading to a zero value when using the initial estimates retrieved by the SIMPLISMA-based algorithm. In contrast, when using EFA and TDA-CAM-B3LYP initialization strategies, the concentration of the acid species does not reach a zero value in the center of the bolus. The latter results are in agreement with those obtained by MCR-ALS resolution after initialization with the reference spectra of the pure components, which is considered as the true concentration profile. It should be noticed that the experimental conditions determine the shape of the time profile, especially the extension of the alkaline range in the center of the FI peak, since it is possible to modulate the pH-gradient by changing the injection volume, carrier flow or capillary length.

4. Conclusions

In this work, a new strategy for obtaining initial estimates of spectral profiles was demonstrated for the MCR-ALS analysis of absorption spectral-pH data in the acid-base equilibrium of pNP. The TDA-CAM-B3LYP method, with appropriate broadening and shifting parameters, is recommended to obtain adequate simulated spectra than can be used as initial estimates.

Different strategies for the ALS initialization, which had influence on the final results, were evaluated. The best resolutions were obtained when the TDA-CAM-B3LYP simulation or EFA algorithm were used to generate the initial estimates. In this particular case, the initial estimates retrieved by the SIMPLISMA-based algorithm led to unsatisfactory results, while the good performance of the TDA-CAM-B3LYP simulated spectra to retrieve reliable results was confirmed.

Besides, it was proved that computational chemistry can be successfully applied as an additional method for obtaining initial estimates in MCR-ALS analyses. In sum, the combination of experimental and theoretical methods is a powerful tool for the acquisition of valuable knowledge about the system under study.

Author contributions

The manuscript was written through contributions of all authors. All authors have given approval to the final version of the manuscript.

Notes

The authors declare no competing financial interest.

Acknowledgments

Prof. Walter M. F. Fabian (Karl-Franzens Universität Graz, Austria) is gratefully acknowledged for helpful discussions.

This work was supported by the Austrian Academic Exchange Service (ÖAD, AR 06/2015) and Ministerio de Ciencia, Tecnología e Innovación Productiva (MINCyT, AU/14/12) in the framework of Wissenschaftlich-Technische Zusammenarbeit, CONICET (Project PIP 2015-0111), UNL (Projects CAI + D 2016 50020150100063LI and 50120150100110LI) and ANPCyT (Project PICT 2014-0347).

References

[1] S.C. Rutan, A. de Juan, R. Tauler, Introduction to multivariate curve resolution, in: S.D. Brown, R. Tauler, B. Walczak (Eds.), Comprehensive Chemometrics, Elsevier, Oxford, 2009, pp. 249–259.
[2] A. de Juan, S.C. Rutan, R. Tauler, Two-way data analysis: multivariate curve resolution – iterative resolution methods, in: S.D. Brown, R. Tauler, B. Walczak (Eds.), Comprehensive Chemometrics, Elsevier, Oxford, 2009, pp. 325–344.
[3] R. Tauler, M. Maeder, Two-way data analysis: multivariate curve resolution – error in curve resolution, in: S.D. Brown, R. Tauler, B. Walczak (Eds.), Comprehensive Chemometrics, Elsevier, Oxford, 2009, pp. 345–363.
[4] R. Tauler, M. Maeder, A. de Juan, Multiset data analysis: extended multivariate curve resolution, in: S.D. Brown, R. Tauler, B. Walczak (Eds.), Comprehensive Chemometrics, Elsevier, Oxford, 2009, pp. 473–505.
[5] E. Peré-Trepat, S. Lacorte, R. Tauler, Alternative calibration approaches for LC–MS quantitative determination of coeluted compounds in complex environmental mixtures using multivariate curve resolution, Anal. Chim. Acta 595 (2009) 228–237.
[6] E. Peré-Trepat, R. Tauler, Analysis of environmental samples by application of multivariate curve resolution on fused high-performance liquid chromatography–diode array detection mass spectrometry data, J. Chromatogr. A 1131 (2006) 85–96.
[7] S. Mas, A. de Juan, S. Lacorte, R. Tauler, Photodegradation study of decabromodiphenyl ether by UV spectrophotometry and a hybrid hard- and soft-modelling approach, Anal. Chim. Acta 618 (2008) 18–28.
[8] J. Jaumot, V. Marchán, R. Gargallo, A. Grandas, R. Tauler, Multivariate curve resolution applied to the analysis and resolution of two-dimensional [1H,15N] NMR reaction spectra, Anal. Chem. 76 (2004) 7094–7101.
[9] M.J. Lopez, C. Ariño, S. Díaz-Cruz, J.M. Diaz, R. Tauler, M. Esteban, Voltammetry assisted by multivariate analysis as a tool for speciation of metallothioneins: competitive complexation of α- and β-metallothionein domains with cadmium and zinc, Environ. Sci. Technol. 37 (2003) 5609–5616.
[10] R. Tauler, I. Marqués, E. Casassas, Multivariate curve resolution applied to three-way trilinear data: study of a spectrofluorimetric acid–base titration of salicylic acid at three excitation wavelengths, J. Chemom. 12 (1998) 55–75.
[11] W. Windig, J. Guilment, Interactive self-modeling mixture analysis, Anal. Chem. 63 (1991) 1425–1432.
[12] M. Maeder, A.D. Zuberbuhler, The resolution of overlapping chromatographic peaks by evolving factor analysis, Anal. Chim. Acta 181 (1986) 287–291.
[13] A.-M. Kelterer, G. Uray, W.M. Fabian, Long wavelength absorbing carbostyrils as test cases for different TD-DFT procedures and solvent models, J. Mol. Model. 20 (2014) 2217.
[14] A. Charaf-Eddin, A. Planchat, B. Mennucci, C. Adamo, D. Jacquemin, Choosing a functional for computing absorption and fluorescence band shapes with TD-DFT, J. Chem. Theory Comput. 9 (2013) 2749–2760.
[15] R. Brasca, M.A. Romero, H.C. Goicoechea, A.-M. Kelterer, W.M.F. Fabian, Spectroscopic behavior of loratadine and desloratadine in different aqueous media conditions studied by means of TD-DFT calculations, Spectrochim. Acta A 115 (2013) 250–258.
[16] J.S. Swinehart, Organic Chemistry: An Experimental Approach, Appleton-Century-Crofts, New York, 1969.
[17] H. Becker, W. Berger, G. Domschke, Organicum: Practical Handbook of Organic Chemistry, Addison-Wesley Longman, Incorporated, California, 1973.
[18] A.D. Becke, Density-functional thermochemistry. III. The role of exact exchange, J. Chem. Phys. 98 (1993) 5648–5652.
[19] F. Weigend, R. Ahlrichs, Balanced basis sets of split valence, triple zeta valence and quadruple zeta valence quality for H to Rn: design an assessment of accuracy, Phys. Chem. Chem. Phys. 7 (2005) 3297–3305.
[20] R.A. Kendall, H.A. Früchtl, The impact of the resolution of the identity approximate integral method on modern ab initio algorithm development, Theor. Chem. Accounts 97 (1997) 158–163.
[21] M. Head-Gordon, J.A. Pople, M.J. Frisch, MP2 energy evaluation by direct methods, Chem. Phys. Lett. 153 (1988) 503–506.
[22] C. Møller, M.S. Plesset, Note on an approximation treatment for many-electron systems, Phys. Rev. 46 (1934) 0618–0622.
[23] M.W. Schmidt, K.K. Baldridge, J.A. Boatz, S.T. Elbert, M.S. Gordon, J.H. Jensen, S. Koseki, N. Matsunaga, K.A. Nguyen, S. Su, T.L. Windus, M. Dupuis, J.A. Montgomery, General atomic and molecular electronic structure system, J. Comput. Chem. 14 (1993) 1347–1363.
[24] T. Yanai, D. Tew, N. Handy, A new hybrid exchange-correlation functional using the Coulomb-attenuating method (CAM-B3LYP), Chem. Phys. Lett. 393 (2004) 51–57.
[25] S. Sinnecker, A. Rajendran, A. Klamt, M. Diedenhofen, F. Neese, Calculation of solvent shifts on electronic g-tensors with the conductor-like screening model (COSMO) and its self-consistent generalization to real solvents (COSMO-RS), J. Phys. Chem. A 110 (2006) 2235–2245.
[26] A. Klamt, G. Schüürmann, COSMO: a new approach to dielectric screening in solvents with explicit expressions for the screening energy and its gradient, J. Chem. Soc. Perkin Trans. 2 (1993) 799–805.
[27] F. Neese, F. Wennmohs, et al., ORCA: An Ab Initio, DFT and Semiempirical SCFMO Package, Version 2.8, University Bonn, Bonn, Germany, September 2010.
[28] A. Klamt, V. Jonas, T. Buerger, J.C.W. Lohrenz, Refinement and parametrization of COSMO-RS, J. Phys. Chem. A 102 (1998) 5074–5085.
[29] J. Tomasi, M. Persico, Molecular interactions in solution: an overview of methods based on continuous distributions of the solvent, Chem. Rev. 94 (1994) 2027–2094.
[30] T. Petrenko, F. Neese, ORCA_ASA, Version 2.6.35, University of Bonn, Bonn,

Germany, 2008.
[31] T. Petrenko, F. Neese, An efficient and general method for the calculations of absorption and fluorescence bandshapes as well as resonance Raman intensities, J. Chem. Phys. 127 (2007) 164319–164324.
[32] M.J.G. Peach, D.J. Tozer, Overcoming low orbital overlap and triplet instability problems in TD-DFT, J. Phys. Chem. A 116 (2012) 9783–9789.
[33] A.D. Laurent, D. Jacquemin, TD-DFT benchmarks: a review, Int. J. Quantum Chem. 113 (2013) 2019–2039.
[34] A.V. Marenich, C.J. Cramer, D.G. Truhlar, C.A. Guido, B. Mennucci, B. Scalmani, M.J. Frisch, Practical computation of electronic excitation in solution: vertical excitation model, Chem. Sci. 2 (2011) 2143–2161.
[35] M. Garrido, M.S. Larrechi, F.X. Rius, R. Tauler, Calculation of band boundaries of feasible solutions obtained by Multivariate Curve Resolution-Alternating Least Squares of multiple runs of a reaction monitored by NIR spectroscopy, Chemom. Intell. Lab. Syst. 76 (2005) 111–120.
[36] M. Garrido, I. Lázaro, M.S. Larrechi, F.X. Rius, Multivariate resolution of rank-deficient near-infrared spectroscopy data from the reaction of curing epoxy resins using the rank augmentation strategy and multivariate curve resolution alternating least squares approach, Anal. Chim. Acta 515 (2004) 65–73.
[37] L. Woods, R.A. Walker, pH effects on molecular adsorption and solvation of *p*-nitrophenol at silica/aqueous interfaces, J. Phys. Chem. A 117 (2013) 6224–6233.
[38] R.G. Bates, G. Schwarzenbach, Die bestimmung thermodynamischer aciditätskonstanten, Helv. Chim. Acta 37 (1954) 1069–1079.
[39] M. Linder, R. Sundberg, Precision of prediction in second-order calibration, with focus on bilinear regression methods, J. Chemom. 16 (2002) 12–27.
[40] H. Abdollahi, R. Tauler, Uniqueness and rotation ambiguities in multivariate curve resolution methods, Chemom. Intell. Lab. Syst. 108 (2011) 100–111.
[41] A. Checa, R. Oliver, J. Saurina, S. Hernández-Cassou, Flow-injection spectrophotometric determination of reverse transcriptase inhibitors used for acquired immuno deficiency syndrome (AIDS) treatment: focus on strategies for dealing with the background components, Anal. Chim. Acta 572 (2006) 155–164.
[42] A. Checa, V. González Soto, S. Hernández-Cassou, J. Saurina, Fast determination of pKa values of reverse transcriptase inhibitor drugs for AIDS treatment by using pH-gradient flow-injection analysis and multivariate curve resolution, Anal. Chim. Acta 554 (2005) 177–183.
[43] J. Saurina, S. Hernández-Cassou, R. Tauler, A. Izquierdo-Ridorsa, Continuous-flow and flow injection pH gradients for spectrophotometric determinations of mixtures of nucleic acid components, Anal. Chem. 71 (1999) 2215–2220.
[44] J. Saurina, Flow-injection analysis for multi-component determinations of drugs based on chemometric approaches, Trends Anal. Chem. 29 (2010) 1027–1037.
[45] J. Saurina, S. Hernández-Cassou, Quantitative determinations in conventional flow injection analysis based on different chemometric calibration statregies: a review, Anal. Chim. Acta 438 (2001) 335–352.